Solution Properties of Synthetic Polypeptides. XIX. Heat Capacity Measurements on the System of Poly(ϵ-carbobenzyloxy-L-lysine) and *m*-Cresol in the Helix–Coil Transition Region

K. Nakamoto, H. Suga, S. Seki,* A. Teramoto, T. Norisuye, and H. Fujita

Department of Chemistry and Department of Polymer Science, Osaka University, Toyonaka, Japan. *Received June 21, 1974*

ABSTRACT: Changes in heat capacity and optical rotation which accompany the helix–coil transition of poly(ϵ-carbobenzyloxy-L-lysine) in *m*-cresol were measured. The data yielded 4.8 ± 0.2 kJ/mol for the transition enthalpy of the system, regardless of molecular weight and concentration. The transition temperature was estimated to be 297.3°K. With these results taken into account, attempts were made to seek a value of the cooperativity parameter σ which allowed the Zimm–Bragg theory for helix-forming polypeptides to be fitted to the observed values of the transition heat capacity as a function of temperature, and the assignment of 0.27×10^{-2} for $\sigma^{1/2}$ was found to give a satisfactory agreement between theory and experiment. These numerical values for transition enthalpy and $\sigma^{1/2}$ can be compared favorably with 3.9 kJ/mol for the former and 0.25×10^{-2} for the latter, both deduced recently by Matsuoka, *et al.*, from an analysis of transition curves for different chain lengths.

In part XV of this series, Matsuoka, *et al.*,[1] found that poly(ϵ-carbobenzyloxy-L-lysine) (PCBL) in *m*-cresol underwent a very sharp thermal helix–coil transition of the inverse type, and, from a detailed analysis of the helical fraction *vs.* temperature curves for samples of different molecular weights, concluded that this system is characterized by $\Delta H_c \approx 3.9$ kJ/mol and $\sigma^{1/2} \approx 0.25 \times 10^{-2}$. Here ΔH_c is the transition enthalpy at the transition temperature T_c, and σ is the cooperativity parameter in the Zimm–Bragg theory of helix-forming polypeptides.[2] The point to note is that this value of $\sigma^{1/2}$ is much smaller than those of other polypeptide–solvent systems and is responsible for the unusually sharp conformational transition of PCBL in *m*-cresol.

In the present paper, an attempt is made to determine the integral transition enthalpy and σ for the system PCBL–*m*-cresol from heat capacity measurements. Such measurements require a specially designed calorimeter and an experimental skill, because the necessary data must be obtained at high dilution and the excess enthalpy for a coil-to-helix change in polypeptide conformation is small. There is only a limited number of polypeptide–solvent systems for which heat capacity data have actually been measured.[3–8] It is our hope that the experimental results presented below can be a significant addition to the literature on the thermodynamics of dilute polypeptide solutions.

Experimental Section

Samples. Three fractionated samples of PCBL, designated L22, L32, and L62, were chosen from our stock[1] for the present work. Their average molecular weights are given in Table I. Each of these samples was freeze dried from a dioxane solution, followed by drying for 48 hr at *ca.* 0.1 Pa and room temperature.

The solvent *m*-cresol was distilled under a nitrogen atmosphere, and the fractions boiling at 59–62° (*ca.* 0.2 kPa) were collected and used immediately.

Each test solution was prepared in such a way that an accurately weighed polypeptide sample was allowed to swell in the solvent of about 45 cm^3 for 1 to 2 days and then brought to complete dissolution with stirring.

Calorimetric Measurement. Use was made of an adiabatic calorimeter designed and described in detail by Suga and Seki.[9,10] A brief account of it is given below for the sake of reference.

Figure 1 shows schematically the calorimeter used. The apparatus was operated with the mode of intermittent energy input with temperature equilibration between successive energizing intervals. The calorimeter cell, its capacity being approximately 41 cm^3, was made of 18-carat gold sheet with eight platinum fins in order to avoid chemical reaction with the solvent. A reentrant well served to hold a heater and a platinum resistance thermometer which had been calibrated on the basis of IPTS-68.

The cell assembly was suspended inside an inner adiabatic shield, which in turn was surrounded by an outer adiabatic shield and an auxiliary block. The temperatures of these shields were controlled by use of a four-channel automatic controller in conjunction with thermopiles. Natural heat leakage to the calorimeter cell was about 10 $\mu J\ sec^{-1}$ when estimated from the temperature drift of the empty cell in a separate series of measurements under the identical conditions. The electric energy supplied to the cell was measured by a Hewlett-Packard seven-place integrating digital voltmeter (3462A) and a Takeda Riken six-place time interval meter (TR-5766U). Resistances of the platinum thermometer were read by a Leeds & Northrup Müller bridge (G2) and a galvanometer.

With about 35 g of solution in each run, the measurements were performed at intervals of 1.0–1.2°K over the temperature range from 285 to 310°K. Equilibration was attained within less than 6 min in the whole temperature range. The measurements were repeated three or four times in order to ensure the reproducibility of thermal anomaly.

Data were taken on five solutions: L22 (0.05378), L32 (0.07612), L62 (0.09153), L62 (0.1675), and L62 (0.2224). The number that follows the sample code indicates the concentration of the solution, m', expressed as the number of moles of monomer unit per kilogram of *solution*.

Optical Rotation Measurement. Optical rotatory angles at the wavelength of 436 nm were measured by use of a Jasco Model DIP-SL automatic recording polarimeter equipped with a quartz cell 10 cm long and 10 mm thick. Data were taken at $m' \approx 0.19$ mol kg^{-1} for the three samples and also at two higher concentrations for sample L62, over the same temperature range as in the heat capacity measurements.

Results

Heat Capacity. Table II presents complete numerical data from the calorimetric measurements.

Figure 2 depicts observed values of C_s at $m' = 0.05376$ mol kg^{-1} for a solution of sample L22 as a function of absolute temperature T. Here the symbol C_s denotes the heat capacity per kilogram of solution at saturation pressure. For comparison, the corresponding values of specific rotation at 436 nm ($[\alpha]_{436}$) are plotted in the lower half of the figure. It is seen that the coil-to-helix transition completes within a range of about 8°K, which indeed means an unusually sharp thermal transition and confirms the similar observations of Matsuoka, *et al.*[1] Because of this feature there was little ambiguity in drawing the base line (dashed line in Figure 2) which connects smoothly the upper and

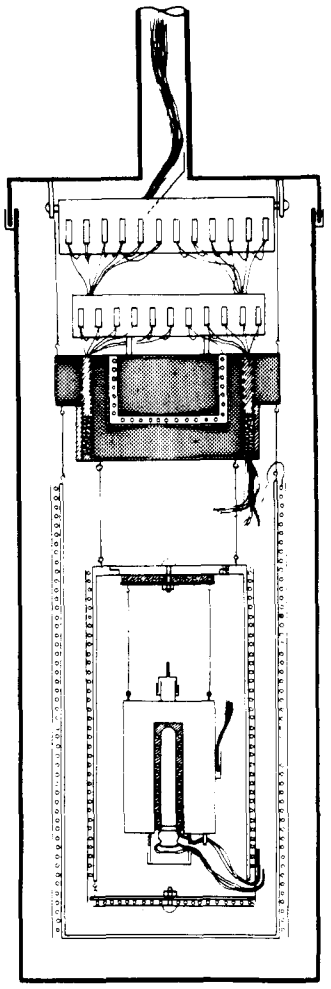

Figure 1. Diagram of the adiabatic calorimeter used.

Table I
Molecular Weights of the Samples Used[a]

Sample code	$\bar{M}_n \times 10^{-4}$	$\bar{M}_w \times 10^{-4}$
L22	27.0	87
L32		41.1
L62		14.4

[a] Taken from ref 1.

lower tails of a C_s *vs.* T curve. The transition (or excess) heat capacity per mole of monomer unit, ΔC_s, may be obtained as $[(C_s)_{obsd} - (C_s)_{base}]/m'$.

Figure 3 shows plots of ΔC_s so obtained against T for L22 (0.05378), L32 (0.07612), and L62 (0.09153), respectively. Since, as will be shown below, the effect of concentration on ΔC_s was quite small, this graph may be taken to indicate that the transition becomes sharper as the chain length of the polypeptide is increased, as should be expected from the theory of helix-forming polypeptides.[2]

Figure 4 illustrates with the data for sample L62 how the curve of ΔC_s *vs.* T is affected by the concentration of the solute. It is observed that the transition shifts to the region of lower temperature and, at the same time, the peak in ΔC_s is lowered as the concentration becomes higher. However, the extents of these effects are small.

An "apparent" transition enthalpy per mole of monomer unit, ΔH_{app}, may be defined as the heat obtained by integrating a ΔC_s *vs.* T curve over the temperature range from T_i to T_f. Here T_i and T_f are the temperatures which are

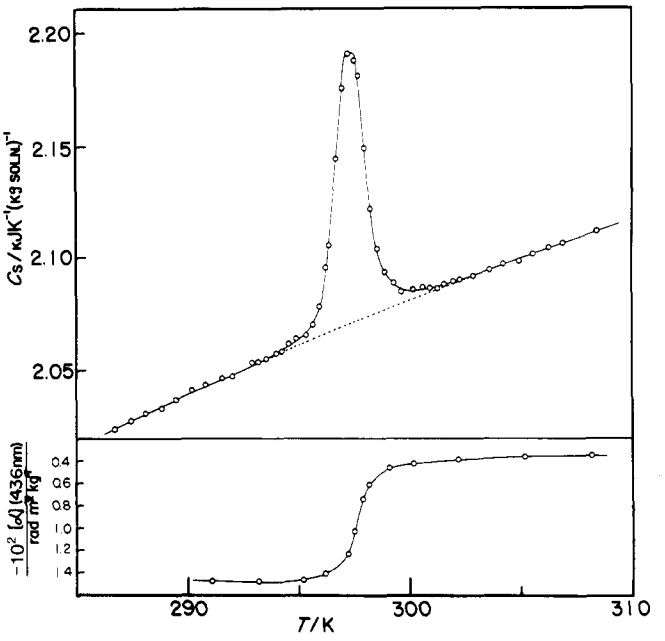

Figure 2. Heat capacity C_s (at saturation pressure) and specific rotation at the wavelength of 436 nm, $[\alpha]_{436}$, for sample L22 at m' = 0.05378 mol kg^{-1}.

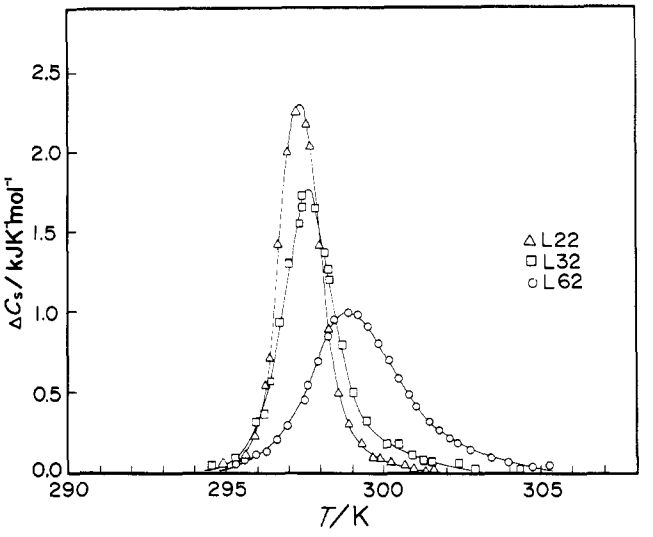

Figure 3. Transition heat capacity ΔC_s (at saturation pressure) as a function of temperature in three solutions: L22 (0.05378), △; L32 (0.07612), □; L62 (0.09153), ○.

located on the random coil side and helix side of the curve considered. Alternatively, ΔH_{app} may be determined from the relation

$$\Delta H_{app} = (\Delta q - \Delta q_{base})/m' \quad (1)$$

where Δq is the heat required to raise the temperature of 1 kg of a given polypeptide solution from T_i to T_f, Δq_{base} is the area of the shadowed region in Figure 5, and m' is the concentration as defined above. Note that Δq may be measured very accurately. Since, in the present measurements, relatively large temperature intervals (1.0–1.2°K) were used to determine individual C_s despite the fact that the transition occurred in a very narrow temperature range, it was considered more accurate to evaluate ΔH_{app} by means of eq 1. The values of ΔH_{app} so obtained for the five solutions studied are given in the third column of Table III.

Optical Rotation. Observed values of $[\alpha]_{436}$ were con-

Table II
Experimental Data for Heat Capacity

T, °K.	C_s,[a] kJ °K^{-1} (kg soln)$^{-1}$	T, °K	C_s, kJ °K^{-1} (kg soln)$^{-1}$	T, °K	C_s,[a] kJ °K^{-1} (kg soln)$^{-1}$	T, °K	C_s, kJ °K^{-1} (kg soln)$^{-1}$
L22 (m' = 0.05378[b])		L32 (m' = 0.07612)		295.96	2.0727	295.00	2.0648
286.69	2.0240	285.99	2.0179	296.29	2.0757	295.50	2.0782
287.43	2.0279	287.73	2.0280	296.63	2.0835	296.04	2.1124
288.07	2.0310	289.47	2.0382	296.97	2.0928	296.53	2.1259
288.81	2.0332	291.05	2.0417	297.49	2.1093	296.82	2.1467
289.44	2.0371	291.71	2.0437	297.60	2.1181	297.05	2.1630
290.18	2.0413	292.48	2.0476	297.93	2.1329	297.53	2.1956
290.81	2.0438	293.14	2.0516	298.26	2.1478	297.82	2.2078
291.55	2.0464	293.91	2.0559	298.46	2.1579	298.04	2.2140
292.01	2.0473	294.56	2.0599	298.90	2.1633	298.52	2.2116
292.92	2.0540	295.33	2.0668	299.21	2.1637	298.81	2.2001
293.20	2.0536	295.39	2.0668	299.53	2.1577	299.03	2.1933
293.54	2.0548	295.47	2.0667	299.87	2.1502	299.51	2.1711
293.99	2.0574	295.97	2.0865	300.18	2.1417	300.03	2.1491
294.28	2.0586	296.25	2.0910	300.49	2.1329	300.51	2.1323
294.57	2.0616	296.43	2.1069	300.82	2.1255	301.04	2.1199
294.90	2.0639	296.43	2.1059	301.05	2.1196	301.53	2.1067
295.35	2.0656	296.74	2.1363	301.47	2.1125	302.07	2.0962
295.63	2.0702	297.02	2.1641	301.78	2.1098	302.55	2.0980
295.93	2.0782	297.36	2.1839	302.11	2.1062	303.10	2.0960
296.25	2.0956	297.38	2.1924	302.36	2.1045	303.58	2.0945
296.38	2.1055	297.41	2.1978	302.78	2.1019	304.13	2.0932
296.68	2.1444	297.85	2.1932	303.41	2.1006	304.39	2.0921
296.96	2.1755	298.10	2.1739	303.97	2.0999	304.61	2.0922
297.25	2.1909	298.24	2.1667	304.71	2.1005	305.16	2.0929
297.57	2.1877	298.27	2.1618	305.27	2.1034	305.43	2.0943
297.69	2.1812	298.69	2.1309	306.01	2.1040	306.19	2.0960
297.99	2.1492	298.73	2.1332	307.31	2.1079	306.47	2.0952
298.27	2.1218	298.81	2.1321	307.41	2.1062	307.50	2.0975
298.56	2.1037	299.08	2.1115	308.46	2.1111	308.54	2.1025
298.89	2.0934	299.46	2.1026	309.52	2.1137	309.58	2.1065
299.32	2.0888	299.49	2.1009	310.57	2.1182	310.62	2.1110
299.66	2.0847	300.12	2.0928	311.62	2.1211	311.65	2.1118
300.22	2.0855	300.51	2.0942	312.67	2.1259	312.68	2.1192
300.66	2.0867	300.89	2.0903	L62 (m' = 0.2224)		L62 (m' = 0.2224)	
300.95	2.0863	301.25	2.0890	285.92	2.0054	298.61	2.2115
301.29	2.0861	301.52	2.0894	287.20	2.0123	299.26	2.1773
301.57	2.0881	302.39	2.0920	288.46	2.0178	299.41	2.1704
301.99	2.0893	302.92	2.0907	288.73	2.0189	299.81	2.1521
302.30	2.0901	304.32	2.0958	289.69	2.0231	300.47	2.1266
302.91	2.0915	304.44	2.0949	290.00	2.0240	300.68	2.1202
303.63	2.0945	305.71	2.0987	290.91	2.0309	301.03	2.1087
304.25	2.0971	306.49	2.1013	291.28	2.0309	301.70	2.0990
304.97	2.0982	307.10	2.1031	292.07	2.0351	302.27	2.0937
305.58	2.1016	308.53	2.1083	292.55	2.0388	302.99	2.0898
306.31	2.1040	310.39	2.1157	293.21	2.0453	303.51	2.0879
306.92	2.1062	312.08	2.1213	293.50	2.0476	304.19	2.0882
308.41	2.1117			293.76	2.0519	304.75	2.0883
L62 (m' = 0.09153)		L62 (m' = 0.1675)		294.13	2.0573	305.43	2.0881
287.95	2.0289	287.05	2.0155	294.44	2.0662	305.99	2.0906
289.10	2.0332	288.13	2.0194	295.01	2.0833	306.67	2.0906
290.34	2.0394	289.20	2.0259	295.05	2.0876	307.20	2.0913
290.97	2.0413	290.25	2.0301	295.68	2.1261	307.23	2.0927
291.67	2.0450	290.77	2.0322	296.16	2.1626	307.91	2.0941
292.31	2.0487	291.31	2.0355	296.24	2.1687	308.44	2.0952
293.00	2.0519	291.83	2.0373	296.89	2.2168	309.68	2.0999
293.64	2.0526	292.37	2.0407	297.19	2.2330	310.92	2.1034
294.33	2.0582	292.90	2.0400	297.43	2.2379	312.15	2.1073
294.97	2.0633	293.42	2.0451	298.07	2.2326	313.39	2.1096
295.32	2.0650	293.95	2.0512	298.27	2.2263		
295.60	2.0686	294.46	2.0574				

[a] Heat capacity (at saturation pressure) per kilogram of solution. [b] Moles of monomer unit per kilogram of solution.

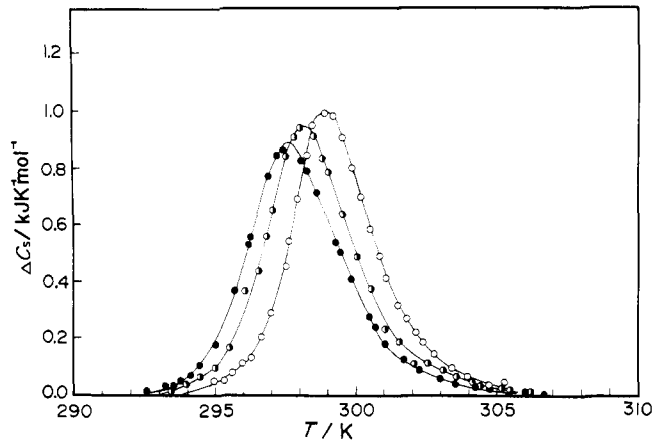

Figure 4. Concentration dependence of ΔC_s plotted against temperature for sample L62: ○, m' = 0.09153 mol kg^{-1}; ◑, m' = 0.1675 mol kg^{-1}; ●, m' = 0.2224 mol kg^{-1}.

Table III
Summary of Important Observed Quantities

Sample code	m', mol kg^{-1}	ΔH_{app}, kJ mol^{-1}	T_{cN},[a] °K	f_m	ΔH_c,[b] kJ mol^{-1}
L22	0.05378	3.96 ± 0.17	297.3	0.84	4.71 ± 0.23
L32	0.07612	3.92 ± 0.15	297.7	0.82	4.78 ± 0.20
L62	0.09153	3.81 ± 0.12	298.9	0.79	4.79 ± 0.23
L62	0.1675	3.82 ± 0.17	298.1		
L62	0.2224	3.74 ± 0.10	297.6		
					Mean 4.76 ± 0.23

[a] Temperature for the maximum in ΔC_s. [b] $\Delta H_c = \Delta H_{app}/f_m$.

verted to helical fractions f_N by the use of an empirical relation established in part XV of this series,[1] *i.e.*

$$f_N = (100[\alpha]_{436} + 1.517)/1.384 \quad (2)$$

Figure 6 shows the f_N *vs.* T so determined for three solutions L22 (0.01703), L32 (0.01992), and L62 (0.01922). The dependence of these curves on chain length conforms qualitatively to the theoretical prediction,[2] but the important point is that each curve levels off at a helical fraction far lower than unity on its helix side. The maximum helical fractions f_m are given in the fifth column of Table III. These low values of f_m originate from the fact that Matsuoka, *et al.*,[1] assigned a rather high value to the magnitude of $[\alpha]_{436}$ for perfectly helical PCBL. A more recent study[11] in our laboratory has indicated that a somewhat smaller value should be chosen for this magnitude in order to interpret more reasonably the results from dielectric measurements on PCBL in *m*-cresol. If eq 2 is modified on the basis of such choice, the present data for $[\alpha]_{436}$ yield values of f_m much closer to unity.

Figure 7 presents the f_N *vs.* T curves for sample L62 at two different values of m'. It is seen that the transition slightly shifts to lower temperature but f_m stays constant within experimental errors as the concentration is increased.

Discussion

If the transition enthalpy is denoted by ΔH, the apparent transition enthalpy can be represented by[13]

$$\Delta H_{app} = \int_{T_i}^{T_f} \Delta H(df_N/dT)dT = \int_0^{f_m} \Delta H df_N \quad (3)$$

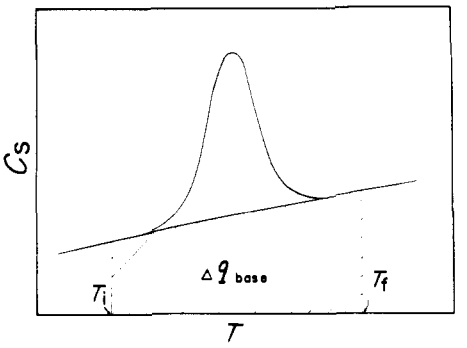

Figure 5. Definitions of T_i, T_f, and Δq_{base}.

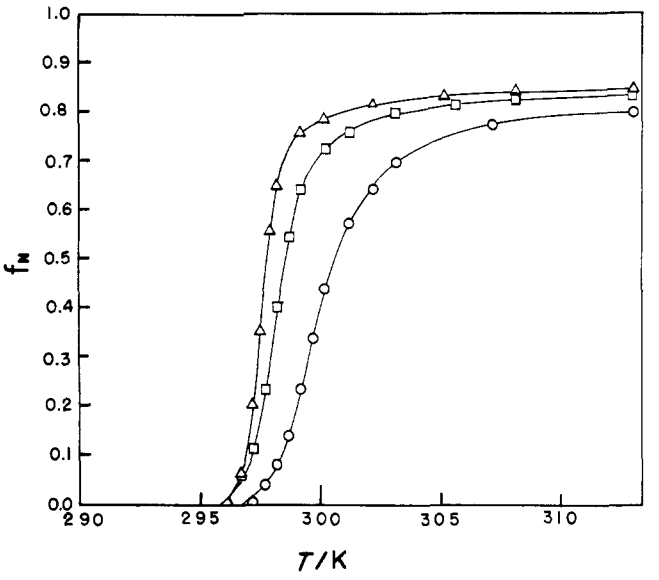

Figure 6. Molecular weight dependence of helical fraction f_N plotted against temperature: Δ, L22 at m' = 0.01703 mol kg^{-1}; □, L32 at m' = 0.01992 mol kg^{-1}; ○, L62 at m' = 0.01922 mol kg^{-1}.

where T_f is chosen as the temperature at which f_N reaches f_m. In general, and especially when the transition is of the inverse type, ΔH depends on temperature.[7] However, if, as in the system under study, the transition takes place in a very narrow range of temperature, ΔH may be equated approximately to ΔH_c, the value of ΔH at the transition temperature T_c. Here T_c is defined as the temperature at which the helical fraction of an infinitely large molecular weight sample becomes one-half. When this approximation holds, eq 3 gives

$$\Delta H_c = \Delta H_{app}/f_m \quad (4)$$

The values of ΔH_c computed from the data given in Table III are listed in the sixth column of the same table. They are essentially independent of molecular weight, yielding 4.8 ± 0.2 kJ/mol as a mean value. This value of ΔH_c is about 20% larger than the one, 3.9 ± 0.5 kJ/mol, obtained by Matsuoka, *et al.*,[1] from an analysis of transition curves, but both should be regarded as being in substantial agreement if we consider the above-mentioned ambiguity in the determination of f_m and the considerable uncertainties that Matsuoka, *et al.*, had to face in fitting the theory to their experimental data. Also, the difficulty in heat capacity measurements at high dilutions must be allowed for.

As has been mentioned above, the f_m values for sample L62 were virtually constant in the concentration range examined. If this fact is coupled with the values of ΔH_{app} given in Table III, we may conclude that the mean value

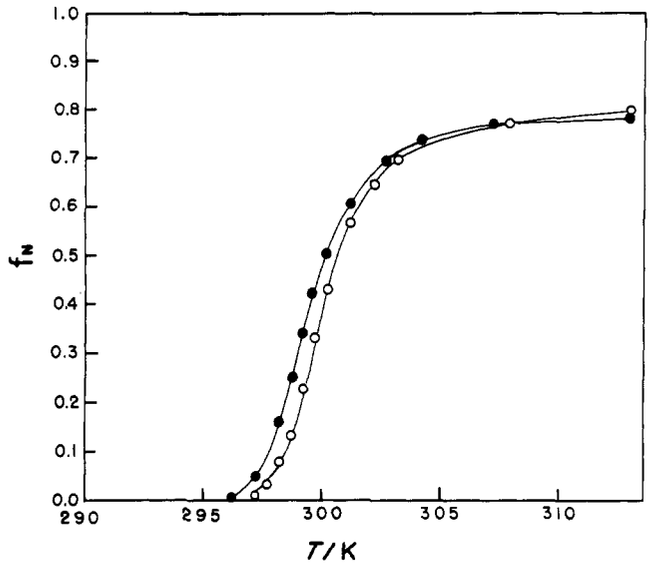

Figure 7. Concentration dependence of f_N plotted against temperature for sample L62: ○, m' = 0.01922 mol kg^{-1}; ●, m' = 0.08674 mol kg^{-1}.

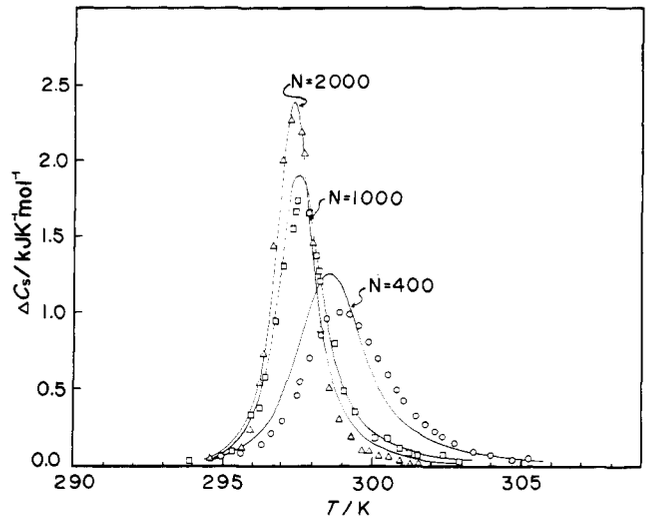

Figure 8. Comparison of calculated and observed values of C_s. Solid lines, computed with T_c = 297.3 K, ΔH_c = 4.76 kJ mol^{-1}, and $\sigma^{1/2} = 0.27 \times 10^{-2}$; N denotes sample's $\bar{N}_n$. Points are experimental values, the symbols having the same meaning as in Figure 3.

for ΔH_c deduced from our calorimetric measurements is independent of solute concentration and thus essentially corresponds to infinite dilution.

The virtual absence of concentration effects in our ΔH_{app} does not conform to the finding by Ackermann and Neumann[5] for poly(γ-benzyl L-glutamate) in mixtures of ethylene dichloride and dichloroacetic acid. They reported a marked decrease of ΔH_{app} with polymer concentration. However, our observations are consistent with the conclusion of Ananthanarayanan, *et al.*,[12] from their differential thermal analysis of poly(γ-benzyl L-glutamate) in a mixture of ethylene dichloride and dichloroacetic acid.

Cooperativity Parameter. The transition heat capacity ΔC_s is related to ΔH by[13]

$$\Delta C_s = \Delta H(\mathrm{d}f_N/\mathrm{d}T) \tag{5}$$

If N (degree of polymerization) $\gg 1$ and $\sigma^{1/2} \ll 1$, f_N can be expressed quite accurately by[14]

$$f_N = f\left\{1 - 2\sqrt{f(1-f)}/(N\sqrt{\sigma}) + [1 + (2\sqrt{f(1-f)}/(N\sqrt{\sigma}))]\exp\left[-\left(\frac{N\sqrt{\sigma}}{\sqrt{f(1-f)}}\right)\right]\right\} \Big/ \left\{1 + \frac{f}{1-f}\exp\left[-\left(\frac{N\sqrt{\sigma}}{\sqrt{f(1-f)}}\right)\right]\right\} \tag{6}$$

Here f is the value of f_N for $N = \infty$ and is given by

$$f = \tfrac{1}{2}[1 + (z/(1 + z^2)^{1/2})] \tag{7}$$

with

$$z = \ln s/(2\sqrt{\sigma}) \tag{8}$$

The quantity s is the Zimm–Bragg variable[2] for the equilibrium constant between random coil and helix units. If the helix–coil transition occurs within so narrow a temperature range that ΔH may be treated as independent of T in the substantial portion of the transition, we have[2]

$$\ln s = -\frac{\Delta H_c}{RT}\left(1 - \frac{T}{T_c}\right) \tag{9}$$

where R is the gas constant, and T_c is the transition temperature, *i.e.*, the value of T at which f becomes one-half or s becomes equal to unity. In this case, ΔH in eq 5 may also be approximated by ΔH_c. Then it is possible to compute from these equations values of ΔC_s as a function of T for a given set of ΔH_c, T_c, σ, and N.

We sought by trial and error a value of σ which would allow the ΔC_s *vs.* T curves calculated in this way to be best fitted to the three sets of experimental data in Figure 3. For this purpose we assigned 4.76 kJ/mol for ΔH_c and 297.3°K for T_c. Actually, the latter is the temperature at which the ΔC_s for the highest molecular weight sample L22 exhibited a maximum. For N in eq 6 we found it relevant to use $\bar{N}_n$ (number-average degree of polymerization), in accordance with the indication of Okita, *et al.*[14] Unfortunately, the necessary $\bar{N}_n$ had been determined only for sample L32, so we tentatively computed those of other samples from their $\bar{M}_w$ with the assumption that $\bar{M}_w/\bar{M}_n$ = 1.4. Evidently, this treatment is a weak point of the present analysis.

The solid lines in Figure 8 depict the results computed with $\sigma^{1/2} = 0.27 \times 10^{-2}$. Their agreement with experimental points is quite good. A better agreement would be obtained if the $\bar{M}_w/\bar{M}_n$ value were adjusted for each sample. The value of $\sigma^{1/2}$ found can be compared favorably with $0.25 \pm 0.06 \times 10^{-2}$ which was derived by Matsuoka, *et al.*,[1] using an entirely different approach.

Summarizing, we find that both ΔH_c and $\sigma^{1/2}$ reported in part XV of this series have been given satisfactory support from calorimetric measurements. It should be noted that precise heat capacity measurements such as done in this work are essential for a direct check of some of the important consequences from the statistical thermodynamic theory of helix-forming polypeptides.

References and Notes

(1) M. Matsuoka, T. Norisuye, A. Teramoto, and H. Fujita, *Biopolymers*, **12**, 1515 (1973).
(2) B. H. Zimm and J. K. Bragg, *J. Chem. Phys.*, **31**, 526 (1959).
(3) Th. Ackermann and H. Rüterjans, *Z. Phys. Chem. (Frankfurt am Main)*, **41**, 116 (1964).
(4) Th. Ackermann and H. Rüterjans, *Ber. Bunsenges. Phys. Chem.*, **68**, 850 (1964).
(5) Th. Ackermann and E. Neumann, *Biopolymers*, **5**, 649 (1967).
(6) F. E. Karasz, J. M. O'Reilly, and H. E. Bair, *Nature (London)*, **202**, 693 (1964).
(7) F. E. Karasz, J. M. O'Reilly, and H. E. Bair, *Biopolymers*, **3**, 241 (1964).
(8) F. E. Karasz and J. M. O'Reilly, *Biopolymers*, **4**, 1015 (1966).
(9) H. Suga and S. Seki, *Bull. Chem. Soc. Jap.*, **38**, 1000 (1965).

(10) O. Haida, T. Matsuo, H. Suga, and S. Seki, *J. Chem. Thermodyn.*, **6**, 3070 (1974).
(11) I. Omura, A. Teramoto, and H. Fujita, *Macromolecules*, submitted for publication.
(12) V. S. Ananthanarayanan, G. Davenport, E. R. Stimson, and H. A. Scheraga, *Macromolecules*, **6**, 559 (1973).
(13) A. Teramoto and T. Norisuye, *Biopolymers*, **11**, 1693 (1972).
(14) K. Okita, A. Teramoto, and H. Fujita, *Biopolymers*, **9**, 717 (1970).

The Determination of an Alternating Monomer Sequence Distribution in Propylene-Butadiene Copolymers Using Carbon-13 Nuclear Magnetic Resonance

Charles J. Carman

The B.F. Goodrich Company Research and Development Center, Brecksville, Ohio 44141.
Received July 12, 1974

ABSTRACT: Pulsed Fourier transformed carbon-13 nuclear magnetic resonance spectra were used to determine that two copolymers of propylene and butadiene made with different catalysts both had a perfectly alternating monomer sequence distribution. The two copolymers were also hydrogenated and the ^{13}C nmr spectra of the resulting polyalkanes were compared to past ^{13}C nmr spectra for branched alkanes and ethylene propylene copolymers. The ^{13}C data are shown to be more sensitive to structure than proton nmr data and clearly exclude the presence of structures with adjacent identical monomers. The ^{13}C nmr spectra of the original copolymers show that a vandium catalyst system produced alternating copolymers with all of the butadiene in a trans configuration. The copolymer made with a titanium catalyst system is also shown to have an alternating structure but with 89% of the butadiene in a trans configuration and 11% in a cis configuration. Low concentrations of polybutadiene homopolymer are detected and quantitatively measured in both polymer systems. The ^{13}C nmr spectra are not useful for determining tacticity in this polymer system.

The synthesis of copolymers of propylene and butadiene with alternating monomer sequence distribution has been reported.[1-5] The strongest evidence for the alternating structure is a 1:1 monomer composition in the copolymer, irrespective of varied composition in the monomer feed. Both infrared (ir) analysis and proton nuclear magnetic resonance (pmr) analysis can be used to determine composition in the polymer. However, unambiguous spectroscopic observation of an alternating monomer sequence structure has not been entirely satisfying. Previous investigators[3] found that it was necessary to use 220 MHz proton nmr spectra to assign an alternating structure to the copolymers. Even so, those data and earlier infrared data[1,2] could only be used to infer an alternating structure. They could not be used to unambiguously exclude the presence of nonalternating structure.

We have found that carbon-13 nuclear magnetic resonance (^{13}C nmr) is a sensitive method for determining the monomer sequence distribution in ethylene propylene copolymers.[6,7] If one would hydrogenate a propylene-butadiene copolymer, the resulting polyalkane would be analogous to a copolymer of ethylene and propylene. If in fact the propylene and butadiene monomers were alternating, the resulting polyalkane would be composed of regular, repeating sequences of five methylene carbons bounded by tertiary carbons each bearing a methyl group. Because of the sensitivity of ^{13}C nmr chemical shifts to methylene sequence lengths in branched alkanes,[8-10] it would be a straightforward task to determine the presence and concentration of sequences coming from nonalternating structures. Furthermore, by combining the chemical shifts for the polyalkane with approximate alkene substituent effects derived from the literature,[13] one could expect to be able to interpret the ^{13}C nmr spectra of the original (nonhydrogenated) copolymers in terms of sequence distribution, as well as be able to determine the cis and trans structure around the olefin bond.

This report demonstrates how ^{13}C nmr can be used to determine the alternating monomer structure for two propylene butadiene copolymers made with different catalysts but both of which are reported to produce an alternating copolymer. The data show how ^{13}C nmr can be used to unambiguously preclude the presence of any nonalternating structure in these copolymers.

Experimental Section

The random-noise, proton decoupled, natural abundance ^{13}C nmr spectra were obtained from the Fourier transform of the free induction decay using a Varian XL-100-15 pulsed nmr spectrometer. All the spectra were obtained at the Major Analytical Instrument Facility at Case Western Reserve University.

Spectra were obtained at ambient probe temperature using 12-mm tubes. The polymers were examined as approximately 20% (w/v) solutions in a 1:1 $CCl_4/CDCl_3$ mixed solvent. The $CDCl_3$ was used for the internal deuterium lock. Internal tetramethylsilane was present in all samples as an internal chemical shift reference. The spectra were obtained using a spectral width of 5000 Hz, 8192 data points, and 0.8 sec acquisition time. The spectra of the propylene-butadiene copolymers were obtained using a 60° pulse. This was achieved using a 35-μsec pulse width for the spectrum shown in Figure 1. (The power amplifier was used to obtain the spectrum shown in Figure 5, consequently the 60° pulse was achieved using an 8-μsec pulse width.) A 30° pulse using a 15-μsec pulse width was used to obtain the spectra of the hydrogenated copolymers. The number of transients accumulated for the spectra shown are as follows: 2500 for Figures 1 and 2; 15,436 for Figure 3; 25,961 for Figure 4; and 2,060 for Figures 5 and 6.

The high molecular weight copolymers of propylene and butadiene were obtained from the Maruzen Petrochemical Co., Ltd. Copolymer A was made with a vanadium catalyst system and copolymer B was made with a titanium catalyst system. The copolymers were hydrogenated using a Raney nickel catalyst, and also using *p*-toluenesulfonylhydrazide.[14] Both methods produce a polyalkane having the same ^{13}C nmr spectra.

Results and Discussion

The ^{13}C nmr spectrum is shown in Figure 1 for a propylene-butadiene copolymer made with a vanadium catalyst that is reported to produce a copolymer with an alternating monomer sequence distribution. The seven resonances were assigned to the structure shown in Figure 1 after comparing the ^{13}C chemical shifts to those found for this co-